Cluster model for radiative transition probabilities of d^5 ions in tetrahedral symmetry: Case of Mn^{2+} in the common cation series ZnS, ZnSe, and ZnTe

D. Boulanger
Université de Paris-Sud, Laboratoire d'Informatique, Maîtrise de Sciences Physiques, Bâtiment 479, 91405 Orsay Cedex, France

R. Parrot
Institut Universitaire de Formation des Maîtres et Institut d'Enseignement Supérieur de Guyane, Boîte Postale 792, 97337 Cayenne Cedex, Guyane Française, France

Z. Cherfi
Université de Technologie de Compiègne, Laboratoire Conception et Qualité des Produits et des Processus, Equipe de Recherche Technologique 19, Boîte Postale 649, 60206 Compiègne, France
(Received 5 January 2004; published 31 August 2004)

A cluster model is proposed to account for the increase of one to almost two orders of magnitude for the radiative transition probabilities (RTP's) of Mn^{2+} in the common cation series ZnS, ZnSe, and ZnTe. First, it is shown that the RTP's of d^5 ions in tetrahedral symmetry are given by second-order perturbation schemes involving the molecular electric dipole moment and the molecular spin-orbit (MSO) interaction. Then, a model is elaborated to calculate the monoelectronic matrix elements of the molecular electric dipole moment and of the MSO interaction. In particular, three methods are proposed to calculate the molecular electric dipole moment. For the studied compounds, the metal-metal, metal-ligand, and ligand-ligand contributions of the group overlaps to the molecular electric dipole moment and to the MSO interaction are analyzed. It is shown that the strong increase of the RTP's when passing from ligands S to ligands Se and Te is primarily controlled by the MSO interaction of the ligands. Then, the radiative lifetimes (RL) for Mn^{2+} in ZnS, ZnSe, and ZnTe, are calculated and found to be in good agreement with the experimental values. Finally, the RL's of Mn^{2+} in other II-VI compounds, and of Mn^{2+} and Fe^{3+} in several III-V compounds are briefly considered.

DOI: 10.1103/PhysRevB.70.075209 PACS number(s): 71.55.Gs, 71.55.Eq, 71.70.Ch, 71.70.Ej

I. INTRODUCTION

The experimental determination of the radiative lifetimes (RL's) of d^5 ions, such as Mn^{2+} and Fe^{3+}, in II-VI (Refs. 1–5) and III-V (Refs. 6–11) compounds has long attracted much attention. Most experiments on RL's have been performed on d^5 ions in cubic or axial crystals.[1–11] However, much attention has also been given to the RL's of Mn^{2+} in nanoclusters (NC's).[12,13]

For example, in the case of $ZnS:Mn^{2+}$ NC's, very short RL's have been observed in the region of the emission of Mn^{2+} and have been related to Mn^{2+} centers.[12] However, very recent time-resolved excitation and emission experiments in small $ZnS:Mn^{2+}$ NC's (mean diameter of 12 Å) have clearly shown that in addition to the fast decays observed in early experiments, a slow decay of 1–2 ms is present and that it is in the range of the RL's of isolated Mn^{2+} centers in ZnS crystals.[13] The slow decay has been attributed to Mn^{2+} centers while the fast decays have been attributed to trap states of ZnS NC's.[13]

In the following, we will consider single crystals in order to elaborate a molecular cluster model for the RL's of d^5 ions in II-VI and III-V compounds since single crystals show much more detailed features than NC's such as a well known symmetry, well defined zero phonon lines, known phonon structures and Jahn-Teller couplings. Of course, the proposed cluster model can be used to interprete the RL's of d^5 ions inside NC's, but cannot be used to analyze centers involving d^5 ions near the surface of NC's. We will now present an overall view of the experimental RL's of d^5 ions in II-VI and III-V crystals and select one set of RL's to elaborate a detailed cluster model.

The radiative lifetimes of the fluorescent $^4T_1$ level of Mn^{2+} and Fe^{3+} have been measured in a variety of II-VI and III-V compounds. In the case of Mn^{2+} in the common cation series: cubic ZnS,[1,2] ZnSe,[3,4] and ZnTe,[5] the RL's decrease from 1.77 ms to 0.22–0.24 ms and 40–52 μs, respectively, thus showing that the RL's of Mn^{2+} is 8 times shorter in ZnSe than in ZnS, and 40 times shorter in ZnTe than in ZnS. In the case of Fe^{3+}, the RL in ZnS[6] (4.3 ms) is six times shorter than in ZnO (Ref. 7) (25.2 ms, axial symmetry). For Fe^{3+} in III-V compounds the RL is four times shorter in GaAs (Refs. 8 and 9) (1.9 ms) than in GaN (Ref. 10) (8 ms). The RL of Fe^{3+} in InP is of 1.1 ms.[11]

Concerning the fluorescent levels of d^5 ions, a recent analysis of the fine structures of the $^4T_1$ levels of Mn^{2+} and Fe^{3+} in several II-VI and III-V compounds has shown that, due to the MSO interaction and the Jahn-Teller effect, the fine structures are much more complex than expected from early crystal field (CF) models.[14] In cubic symmetry, the fluorescent $^4T_1$ level of a d^5 ion decomposes into four electronic levels Γ_6, Γ_7, $\Gamma_8(3/2)$ and $\Gamma_8(5/2)$ and the fundamental level into two Γ_7 and Γ_8 levels. As shown in Fig. 1, in the case of ZnS, the four fine structure lines of the fluorescent $^4T_1$ level coalesce into two almost degenerate Γ_7 and $\Gamma_8(3/2)$ levels at lower energy separated by 9.7 cm^{-1} from two al-

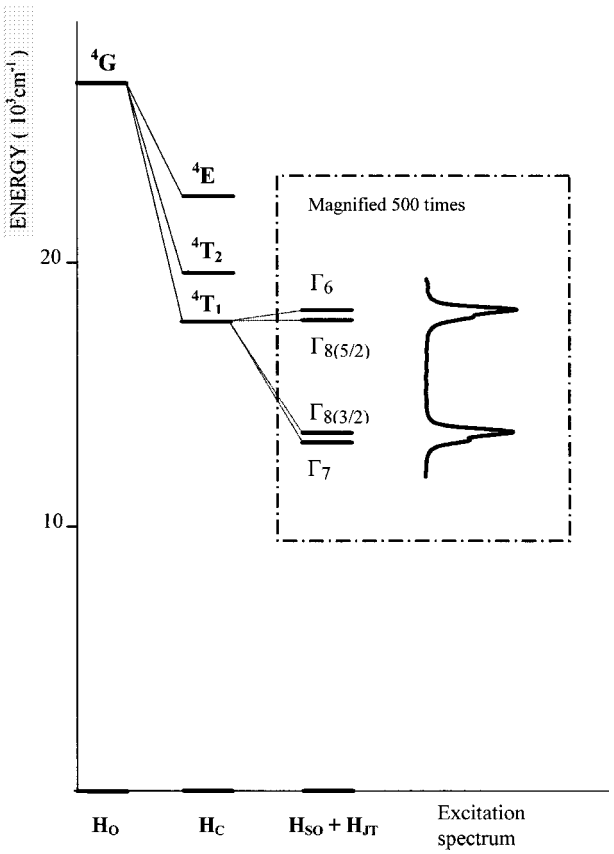

FIG. 1. Energy levels at lower energy of Mn^{2+} in cubic symmetry. The spectroscopic ^4G term and three multiplets are represented to the left. The experimental and theoretical fine structures of the fluorescent level as observed in ZnS are given in the inset. H_0, H_C, H_{SO}, and H_{JT} represent the free ion Hamiltonian, the cubic field interaction, the spin-orbit interaction, and the Jahn-Teller interaction, the splitting of the fundamental $^6A_1$ level is not represented.

most degenerate $\Gamma_8(5/2)$ and Γ_6 levels at higher energy. In the case of ZnSe, the two degenerate levels appearing at lower energy are separated by 11.5 cm^{-1} from the two degenerate levels at higher energy. The splittings of the degenerate levels have not been observed experimentally in ZnSe. For ZnTe, the fine structure is not known.

The fundamental $^6A_1$ level decomposes into two levels Γ_7 and Γ_8 with $W(\Gamma_8)-W(\Gamma_7)=3a$, a being the fine structure constant determined from electron paramagnetic resonance experiments. In the model developed here for the RL's, the splitting of the $^6A_1$ level will be neglected since it is of $3a=7.87\times10^{-4}$ cm^{-1}, 19.7×10^{-4} cm^{-1}, and 29.6×10^{-4} cm^{-1} for Mn^2 in ZnS,[15] ZnSe,[15] and ZnTe,[16] respectively.

It has long been realized that, in the crystal-field (CF) model, the large values of RL's characteristic of d^5 ions is due to the fact that the transition from the fluorescent $^4T_1$ level to the fundamental $^6A_1$ level is spin and parity forbidden. The spin interdiction can be removed by using the spin-orbit (SO) interaction. Concerning parity, it is necessary to consider crystal fields of odd parity and electronic configurations of odd parity in order to get non zero matrix elements for the electric dipole moment $e\mathbf{r}$.

In the CF model, the excited configurations $3d^44p$ and $3d^44f$ have long been used to calculate the classical[17] and relativistic[18] electric field effects in $e\mathbf{E}.\mathbf{r}$ on d^5 ions. The RL's of d^5 ions are given by perturbation schemes involving crystal fields of odd parity, the SO interaction, and the electric dipole moment. The RL's depend on the SO coupling constant of the *d* electrons and slightly depend on the ligands *via* the internal crystal field so that the CF model cannot account, for example, for the drastic variations of the RL's in the common cation series ZnS, ZnSe, and ZnTe.

It can be noted here that contrary to the case of d^5 ions, the CF model correctly accounts for the RL's of spin and parity allowed transitions, such as the $5d\rightarrow4f$ transitions of rare-earth ions. For example, the experimental RL's of 36 ns for Ce^{3+} in CaS, 750 ns for Eu^{2+} in CaS, 20 ns for Ce^{3+} in $SrGa_2S_4$, and 580 ns for Eu^{2+} in $SrGa_2S_4$ are correctly accounted for by the CF model used by Hoshina[19] since the theoretical values differ from the experimental values by factors of 0.5 to 3.5 only.

A phenomenological molecular model for the radiative dipole strengths (RDS's) of Mn^{2+} in the common cation series ZnS, ZnSe, and ZnTe has previously been proposed by Boulanger *et al.*[20] to account for the drastic variations of the RL's of Mn^{2+} in II-VI compounds. The model is based on the facts that (i) the transitions between the $|^4T_1\rangle$ state and the fundamental $|^6A_1\rangle$ state are spin forbidden and that this interdiction is removed by the MSO interaction and (ii) the electric dipole transitions are no longer parity forbidden in molecular models, so that, second-order perturbation schemes can account for the RDS's.

It must be noted that the MSO interaction is of primary importance when the SO coupling constants ζ_L of the *p* electrons of the ligands is greater than the SO coupling constants ζ_d of the metal. This is the case for Mn in the considered II-VI compounds, since the ratios ζ_L/ζ_d are approximately of 1, 4.5, and 11.5 for S, Se, and Te, respectively.[21] In fact, the MSO interaction is the fundamental interaction which can account for variations of one to two orders of magnitude for physical coefficients of d^5 ions in crystals. For example, it has been shown that the spin-lattice coupling coefficients (SLCC's) of d^5 ions which describe the coupling of the fundamental level to *E* strains, are strongly dependent on the nature of the ligands and are correctly accounted for by second-order perturbation schemes involving twice the MSO interaction between the fundamental state and the $|^4T_1\rangle$ states.[21]

Concerning the molecular models, it is necessary to check the validity of the monoelectronic and multielectronic wavefunctions by fitting several physical constants. In the case of Mn^{2+} in ZnS and ZnSe, the monoelectronic and multielectronic orbitals have already been tested by calculating the orbit-lattice coupling coefficients (OLCC's) of the $^4T_1$ and $^4T_2$ levels at lower energy.[22] The molecular orbitals as well as the MSO interaction have also been tested by calculating the SLCC's of the $^6A_1$ level of Mn^{2+} in ZnS, ZnSe, and ZnTe (Ref. 21) and the fine structure of the fluorescent $^4T_1$ levels of Mn^{2+} in ZnS and ZnSe.[14]

The aim of this paper is to elaborate a cluster model for the RL's of d^5 ions in tetrahedral symmetry and to perform a molecular calculation of the MSO interaction and of the molecular electric dipole moment in the case of Mn^{2+} in the common cation series ZnS, ZnSe, and ZnTe. The general

definition of the probability of spontaneous emission and the molecular model for the transition probabilities for the emission bands and for the zero phonon lines are presented in Sec. II. The methods used to calculate the MSO interaction, the molecular electric dipole moment, and the transition probabilities are presented in Sec. III. The monoelectronic wave functions for Mn^{2+} in ZnS, ZnSe, and ZnTe, the matrix elements of the MSO interaction, and of the molecular electric dipole moment are given in Sec. IV. Finally, in Sec. V, the theoretical results are presented and compared with the experimental results. The RL's of d^5 ions in II-VI and III-V compounds are briefly considered.

II. TRANSITION PROBABILITIES AND VIBRONIC INTERACTIONS

A. General model

The probability of the spontaneous emission per unit time from an initial state A to a final state B is given by[19,23]

$$P(A,B) = \frac{1}{\tau} = \frac{1}{d_A}\frac{64\pi^4\sigma^3\chi e^2}{3h}S(A,B), \tag{1}$$

where τ is the radiative lifetime, d_A is the degeneracy of the initial state, σ is the energy of the emitted light, χ is a correcting factor which accounts for the effective electric field at the site of the impurity, and $S(A,B)$ is the total line strength of the transition. $S(A,B)$ is given in terms of the components $j=x$, y, or z of the electric dipole moment and in terms of the components a and b of the initial and final states by

$$S(A,B) = \sum_j S_j(A,B) \tag{2}$$

with

$$S_j(A,B) = \sum_a \sum_b S_j(Aa,Bb). \tag{3}$$

We will now consider the operators as well as the electronic and vibronic levels intervening in the calculation of the total line strength $S(A,B)$ for transitions from the fluorescent $^4T_1$ level to the fundamental $^6A_1$ level of d^5 ions in tetrahedral symmetry.

The operators and energy levels involved in molecular second-order perturbation schemes are shown in Fig. 2. In this figure, the first scheme involves intermediate $^4T_1{}^q$ levels, the MSO interaction, and the molecular dipole moment. For the second scheme, the intermediate $^6T_2$ levels are due to the promotion of one electron from a filled inner shell $1t_2$, $1a_1$, $2t_2$, $1e$, $1t_1$, $2a_1$, or $3t_2$ to half-filled shells $4t_2$ or $2e$ or from the promotion of one electron from the half-filled shells $4t_2$ or $2e$ to empty shells $5t_2$ or $3a_1$ appearing at high energy (see Fig. 3). In Fig. 3, the empty shells $5t_2$ and $3a_1$ at high energy are not represented. We can note that $^6T_2$ levels do not exist in a model restricted to the configuration d^5.

In the proposed molecular model, we will consider the contributions of the intermediate $^4T_1{}^q$ ($q=1$, 2, and 3) levels which are built from the configurations $4t_2{}^4 2e$, $4t_2{}^3 2e^2$, and $4t_2{}^2 2e^3$ with two open shells (see Fig. 3) and neglect the contributions of the configurations with three open shells such as the contributions of the $^4T_1$ and $^6T_2$ multiplets which appear at very high energy. It must be noted here, that a molecular calculation restricted to the configurations $4t_2{}^4 2e$, $4t_2{}^3 2e^2$,and $4t_2{}^2 2e^3$ correctly accounted for the SLCC's of Mn^{2+} in the studied compounds.

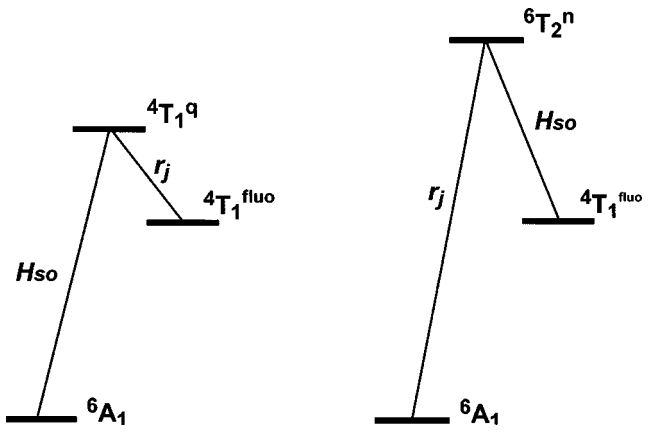

FIG. 2. Second-order perturbation schemes used in the calculation of the RL's. H_{SO} is the MSO interaction, r_j is the component j of $\mathbf{r}$. The $^4T_1$ levels are considered in the scheme to the left. The $^6T_2$ levels appear in configurations with three open shells only.

Concerning the phonons, in T_d symmetry, the electronic

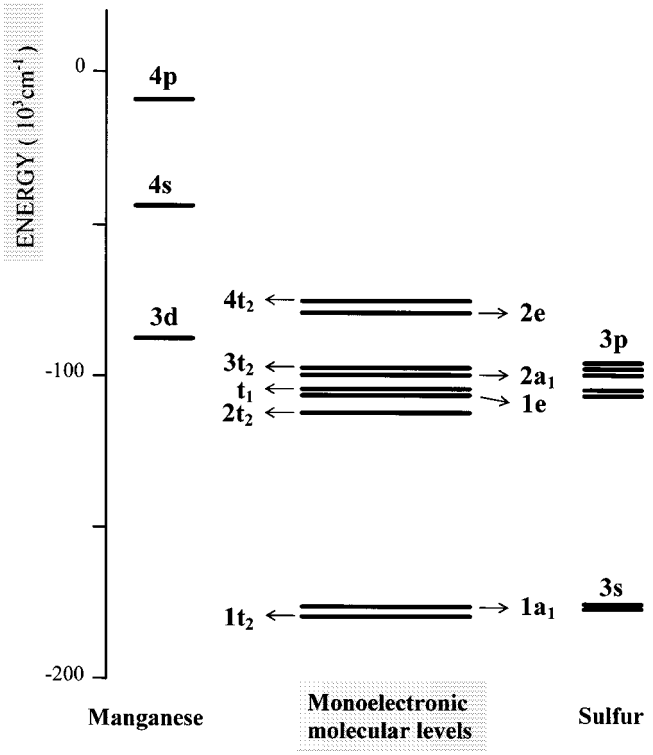

FIG. 3. Monoelectronic energy levels for Mn^{2+} in ZnS for the set a of values for the molecular coefficients. The monoelectronic energy levels of Mn and S are given to the left and to the right, respectively. Several molecular energy levels are given in the center. The levels $4t_2$ and $2e$ are of primary importance to calculate the RL's.

states are coupled to α_1, ε, and τ_2 modes. For the fluorescent levels, in the case of ZnS and ZnSe, the uniaxial stress effect has shown a coupling to A_1 strains and a Jahn-Teller coupling to E strains, the coupling to T_2 strains being either small or strongly reduced by the Jahn-Teller coupling to E strains.[21] The influence of phonons on the second-order perturbation scheme involving the ${}^4T_1$ levels is studied in the case of a coupling to ε modes which is preponderant to account for the fine structure of the fluorescent level.

In the molecular model, the components S_j of the total line strength for transitions ${}^4T_1 \rightarrow {}^6A_1$ involving the ε modes are given in terms of the matrix elements of the MSO interaction and of the matrix elements of the components r_j of the molecular electric dipole moment by

$$S_j\left({}^4T_1 u M_s 00, {}^6A_1 M_{s'} n_\theta' n_\varepsilon'\right) = \left| \sum_{\nu,q} \sum_{n_\theta, n_\varepsilon} \frac{\langle A_1 M_{s'} n_\theta' n_\varepsilon' | H_{\mathrm{SO}} | {}^4T_1^q \nu M_s n_\theta n_\varepsilon \rangle \langle {}^4T_1^q \nu M_s n_\theta n_\varepsilon | r_j | {}^4T_1 u M_s 00 \rangle}{W_{\mathrm{vib}}\left({}^6A_1\right) - W_{\mathrm{vib}}\left({}^4T_1^q\right)} \right|^2. \tag{4}$$

$q=1,2,3$ refers to the three ${}^4T_1$ levels of the d^5 configuration. The ${}^4T_1{}^q$ level with $q=3$ is the fluorescent level which will be simply denoted ${}^4T_1$ in the following. u and v are the orbital components of the ${}^4T_1{}^q$ levels. M_s and $M_{s'}$ are the spin components of the ${}^4T_1$ and ${}^6A_1$ multiplets, respectively. The $|{}^4T_1{}^q \nu M_s n_\theta n_\varepsilon\rangle$ states are vibronic states, whose energies $W_{\mathrm{vib}}({}^4T_1{}^q)$ are given by[24]

$$W_{\mathrm{vib}}\left({}^4T_1^q\right) = W\left({}^4T_1^q\right) + (n_\theta + n_\varepsilon + 1)\hbar\omega - E_{\mathrm{JT}}^q, \tag{5}$$

where $W({}^4T_1{}^q)$ is the energy of the electronic state, $\hbar\omega$ is the energy of an effective phonon of E symmetry, n_θ and n_ε are the number of phonons of E_θ and E_ε symmetry, and E_{JT} is the Jahn-Teller energy of the ${}^4T_1{}^q$ level. The $|{}^6A_1 M_{s'} n_\theta' n_\varepsilon'\rangle$ states are vibronic states of the fundamental ${}^6A_1$ level whose energies are given by

$$W_{\mathrm{vib}}\left({}^6A_1\right) = W\left({}^6A_1\right) + (n_\theta' + n_\varepsilon' + 1)\hbar\omega. \tag{6}$$

Concerning the phonons, the summation on all phonons of the intermediate ${}^4T_1{}^q$ levels can be written as

$$A(n_\theta', n_\varepsilon') = \sum_{n_\theta, n_\varepsilon} \frac{\langle 0 n_\theta' | \nu n_\theta \rangle \langle \nu n_\theta | u 0 \rangle \langle 0 n_\varepsilon' | \nu n_\varepsilon \rangle \langle \nu n_\varepsilon | u 0 \rangle}{W\left({}^4T_1^q\right) - E_{JT}^q - W\left({}^6A_1\right) + (n_\theta + n_\varepsilon - n_\theta' - n_\varepsilon')\hbar\omega}. \tag{7}$$

This sum will intervene in the calculation of the transition probabilities of the zero phonon lines and of the emission band in the following subsection.

B. Transition probability of the ${}^4T_1$ emission band

The transition probability of the ${}^4T_1$ emission band is obtained by summing on all phonons of the fundamental state, so that

$$S_j\left({}^4T_1 u M_s, {}^6A_1 M_{s'}\right) = \sum_{n_\theta', n_\varepsilon'} S_j\left({}^4T_1 u M_s 00, {}^6A_1 M_{s'} n_\theta' n_\varepsilon'\right). \tag{8}$$

By using

$$\sum_{n_\theta', n_\varepsilon'} A(n_\theta', n_\varepsilon')^2 = \frac{1}{\overline{w}(q,\overline{n})^2} \tag{9}$$

we get

$$S_j\left({}^4T_1 u M_s, {}^6A_1 M_{s'}\right) = \left| \sum_q \frac{1}{\overline{w}(q,\overline{n})} \sum_\nu \left\langle {}^6A_1 M_{s'} | H_{\mathrm{SO}} | {}^4T_1^q \nu M_s \right\rangle \times \left\langle {}^4T_1^q \nu M_s | r_j | {}^4T_1 u M_s \right\rangle \right|^2, \tag{10}$$

where

$$\overline{w}(q,\overline{n}) = W\left({}^4T_1^q\right) - W\left({}^6A_1\right) + \overline{n}\hbar\omega. \tag{11}$$

This relation has been calculated from the vibrational wave functions of the ${}^4T_1$ and ${}^6T_1$ levels given by Gélineau.[25] By assuming that $S\hbar\omega$ is identical for the three ${}^4T_1{}^q$ levels, we get $\overline{n}=S$. This result is valid if the energy difference between the ${}^6A_1$ level and the ${}^4T_1{}^q$ levels is much greater than the energy of the phonons as it is the case for Mn^{2+} in II-VI compounds. The values for $\overline{n}$ depend on the Jahn-Teller energies of the levels intervening in the calculation. An analoguous calculation can be used when considering the coupling to α_1 modes. In the following, we will consider that $\overline{w}(q,S) = W_{\mathrm{ZPL}}^q + 2S\hbar\omega$, where W_{ZPL}^q is the the energy of the zero phonon lines, can be approximately given by the energy of the maximum of the absorption bands of the three ${}^4T_1{}^q$ levels.

It can be noted here that the transition probabilites of the ZPL's from the fluorescent level to the ${}^6A_1$ fundamental level are obtained by considering the A_1 level with $n_\theta'=0$ and $n_\varepsilon'=0$, that is $A(0,0)$. For the zero-phonon lines of the fluorescent ${}^4T_1$ level, all transition probabilities are reduced by the factor $\exp(-S)$. Therefore, the Jahn-Teller effect does not modify the relative oscillator strengths of the fine structure lines of the fluorescent ${}^4T_1$ level. Of course, this is not true, when selective intensity transfer occurs as, for example, for the transition ${}^4T_2 \rightarrow {}^6A_1$ of Mn^{2+} in ZnS and ZnSe.[26]

III. MOLECULAR MODEL

A. Molecular spin-orbit interaction

The molecular spin-orbit interaction H_{SO}, which has been defined by Misetich and Buch,[27] can be written as

$$H_{SO} = \sum_i \zeta_M(r_{iM}) \mathbf{l}_M^i \cdot \mathbf{s}^i + \sum_i \sum_L \zeta_L(r_{iL}) \mathbf{l}_L^i \cdot \mathbf{s}^i. \quad (12)$$

The sums are performed on the five electrons i of the configuration d^5 and on the four ligands L. $\mathbf{l}_M^i$ and $\mathbf{l}_L^i$ are one-electron orbital operators for the metal and the ligands, respectively. ζ_M and ζ_L are the spin-orbit coupling constants of the electrons of the metal and ligands, respectively. H_{SO} can conveniently be written in terms of the molecular angular momentum τ_u^i as

$$H_{SO} = \sum_{u,i} \tau_u^i \cdot s_u^i. \quad (13)$$

with

$$\tau_u^i = \zeta_M(r_{iM}) l_{Mu}^i + \zeta_L(r_{iL}) \Omega_u^i, \quad (14)$$

$u=x,y,z$. The Ω_u^i's are the one electron orbital operators for the ligands. The matrix elements of the molecular spin-orbit interaction H_{SO} between the $|^6A_1\rangle$ state and the $|^4T_1\rangle$ states are given by

$$\langle {}^6A_1 M_{s'} | H_{SO} | {}^4T_1^q \nu M_s \rangle = C_{^4T_1}(M_{s'}, M_s) \langle {}^6A_1 | \tau_\nu | {}^4T_1^q \nu \rangle, \quad (15)$$

where the matrix elements $C_{^4T_1}$ give the spin components of H_{SO} between the $^6A_1$ level and the $^4T_1$ levels for a configuration with two open shells. These matrix elements have previously been defined in the strong field complex basis and used to calculate the SLCC's of Mn^{2+} in ZnS, ZnSe, and ZnTe.[21]

B. Molecular electric dipole moment and transition probabilities

The multielectronic $|^4T_1{}^q\rangle$ states are defined on the real basis in the strong field scheme, restricted to the configuration d^5. The matrix elements of the orbital moment τ are identical for $\nu=x$, y, or z, but depend on q. They include the SO coupling constants ζ_M and ζ_L of the metal and of the ligands, respectively.

The matrix elements of r_j of the electric dipole moment between electronic states are calculated in the strong field scheme. On a real basis, the matrix elements of r_j are real, and, by using Griffith's results,[28] it can be shown that they are non-zero only if u, ν, and j are all different. The matrix elements of r_j are also independent of M_s and are invariant for any permutation of u, ν, and j, so that, the sum on ν is reduced to only one term.

It is now possible to perform the sum on the spin components M_s and $M_{s'}$ of the $^4T_1$ and $^6A_1$ levels, respectively. By noting that

$$\sum_{M_s} \sum_{M_{s'}} |C_{^4T_1}(M_{s'}, M_s)|^2 = 1, \quad (16)$$

we obtain

$$S_j({}^4T_1 u, {}^6A_1) = \sum_{M_{s'}, M_s} S_j({}^4T_1 u M_s, {}^6A_1 M_{s'}) = \left| \sum_q \frac{1}{\overline{w}(q,S)} \langle {}^6A_1 | \tau_\nu | {}^4T_1^q \nu \rangle \langle {}^4T_1^q \nu | r_j | {}^4T_1^q u \rangle \right|^2, \quad (17)$$

where ν is different from u and j. If j is different from u, then, the dipole strength $S_j(^4T_1, {}^6A_1)$ of the transition from the fluorescent level to the $^6A_1$ fundamental level is nonzero and its value is independent of j and u, so that

$$S({}^4T_1, {}^6A_1) = \sum_{j,u} S_j({}^4T_1 u, {}^6A_1) = 6f^2 \quad (18)$$

with

$$f = \sum_q \frac{-i}{\overline{w}(q,S)} \langle {}^6A_1 | \tau_z | {}^4T_1^q z \rangle \langle {}^4T_1^q x | z | {}^4T_1 y \rangle. \quad (19)$$

f is real and its value depends of the contribution of the three $^4T_1$ levels from the mixing parameters a_t^q:

$$|{}^4T_1^q u\rangle = a_1^q |{}^4T_1 u(t_2{}^4 e)\rangle + a_2^q |{}^4T_1 u(t_2{}^3 e^2)\rangle + a_3^q |{}^4T_1 u(t_2{}^2 e^3)\rangle, \quad (20)$$

therefore,

$$f = \sum_q \frac{-i}{\overline{w}(q,S)} \sum_{t=1}^{3} \sum_{t'=1}^{3} \sum_{t''=1}^{3} a_t^q a_{t'}^q a_{t''} \langle {}^6A_1 | \tau_z | {}^4T_1 z(t_2{}^{5-t} e^t) \rangle \times \langle {}^4T_1 x(t_2{}^{5-t'} e^{t'}) | z | {}^4T_1 y(t_2{}^{5-t''} e^{t''}) \rangle, \quad (21)$$

where $\overline{w}(q,S)$ is the energy of the maximum of the absorption band of each $^4T_1$ level.

The matrix elements of the repulsive electrostatic interaction are calculated by using the $^4T_1$ triplet states developed in terms of Slater determinants defined in Ref. 22. The mixing parameters of the three $^4T_1$ levels are obtained by diagonalizing the matrix of Sugano *et al.*[29] whose matrix elements are calculated from the Racah parameters B, C, and the cubic-field parameter D_q.

The matrix elements of τ as given in Table I a, depend on the two coefficients ζ_{t2t2} and ζ_{et2}. ζ_{t2t2} is the spin-orbit coupling coefficient between two monoelectronic orbitals t_2 and ζ_{et2} is the spin-orbit coupling coefficient between two monoelectronic orbitals e and t_2. The matrix elements r_{t2t2} and r_{et2} of $\mathbf{r}$ are given in Table I b.

IV. MOLECULAR MODEL FOR THE RL'S OF Mn^{2+} IN II-VI COMPOUNDS

A. Molecular orbitals

For Mn^{2+} in II-VI compounds (see Fig. 3), the molecular orbitals in T_d symmetry have been determined in Ref. 22 from a semiempirical self-consistent method. The calculation was an extension of the method proposed by Ballhausen and Gray[30] and by Buch and Gelineau.[31] The coordinate system is given in Ref. 22, for Mn and its four neighbors.

The atomic radial functions were those calculated by Richardson *et al.*[32] for manganese and by Watson *et al.*[33] for

TABLE I. Multielectronic matrix elements of the z components of $\mathbf{r}$ (a) and τ (b) in terms of the matrix elements $z_{t_2t_2}$, z_{et_2}, $\zeta_{t_2t_2}$, and ζ_{et_2} defined in Secs. IV B and IV C.

a

$\langle {}^4T_1 x(t_2^{5-t'}e^{t'})\lvert z\rvert {}^4T_1 y(t_2^{5-t''}e^{t''})\rangle =$	${}^4T_1(t_2^4e)$	${}^4T_1(t_2^3e^2)$	${}^4T_1(t_2^2e^3)$
${}^4T_1(t_2^4e)$	$-z_{t2t2}/2$	$-z_{et2}/\sqrt{2}$	0
${}^4T_1(t_2^3e^2)$	$-z_{et2}/\sqrt{2}$	0	$z_{et2}/\sqrt{2}$
${}^4T_1(t_2^2e^3)$	0	$z_{et2}/\sqrt{2}$	$z_{t2t2}/2$

b

$\langle {}^6A_1(t_2^3e^2)\lvert \tau_z\rvert {}^4T_1 z(t_2^{5-t''}e^{t''})\rangle =$	${}^4T_1(t_2^4e)$	${}^4T_1(t_2^3e^2)$	${}^4T_1(t_2^2e^3)$
${}^6A_1(t_2^3e^2)$	$2i\zeta et_2$	$-i\sqrt{2}\zeta t_2t_2$	$2i\zeta et_2$

sulfur, and by Clementi[34] for selenium and tellurium. It must be noted here that the radial part of the wavefunctions of the orbitals $3d$ and $4p$ depend on the effective charge Q_M of the metal so that the metal-ligands overlap integrals also depend on Q_M.

For Mn, the valence state ionization potentials (VSIE's) have been calculated following the method proposed by Basch, Viste, and Gray.[35] For sulfur, selenium and tellurium, the following VSIE's have been calculated from the energy levels given by Moore.[36] For sulfur, VSIE$(3s)=-1.77\ Q_L^2+74.13\ Q_L+166.7$ and VSIE$(3p)=7.95\ Q_L^2+83.75\ Q_L+93.4$. For selenium, VSIE$(4s)=6.9\ Q_L^2+91\ Q_L+168$ and VSIE$(4p)=6.9\ Q_L^2+73\ Q_L+87$. For tellurium VSIE$(5s)=3.73\ Q_L^2+98\ Q_L+167.6$ and VSIE$(5p)=7.40\ Q_L^2+76\ Q_L+89.4$.

The off-diagonal matrix elements have been obtained from Cusach's approximation.[37] The influence of the crystal was otained by calculating the diagonal and off-diagonal matrix elements of the electrostatic field due to the first and second nearest neighbors of Mn. The influence on Mn of the other atoms of the crystal was approximated as being their contribution to the Madelung's energy. For the ligands, the influence of the crystal was calculated from the same method.

We will now consider the monoelectronic molecular orbitals $2e$ and $4t_2$ (which will be denoted e and t_2) of two half-filled shells. These monoelectronic molecular orbitals e and t_2 are linear combinations of the atomic orbitals $3d$ and $4p$ of Mn, and of the orbitals $n\sigma s$, $n\sigma p$, and $n\pi p$ ($n=3$ for S, 4 for Se, and 5 for Te) of the ligands:

$$|e_\gamma\rangle = \sum_k b^{Ok}|O_k e_{\gamma'}\rangle = b^d|de_{\gamma'}\rangle + b^{\pi p}|\pi p e_{\gamma'}\rangle, \tag{22}$$

$$|t_{2\gamma}\rangle = \sum_j a^{Oj}|O_j t_{2\gamma}\rangle = a^d|dt_{2\gamma}\rangle + a^p|pt_{2\gamma}\rangle + a^{\sigma s}|\sigma s t_{2\gamma}\rangle + a^{\sigma p}|\sigma p t_{2\gamma}\rangle + a^{\pi p}|\pi p t_{2\gamma}\rangle, \tag{23}$$

$\gamma'=\theta,\varepsilon$ and $\gamma=\xi,\eta$. ζ refers to the components of the e and t_2 orbitals respectively. The values of the coefficients a^d, a^p, $a^{\sigma s}$, $a^{\sigma p}$, $a^{\pi p}$, b^d, and $b^{\pi p}$ are obtained from the semiempirical self-consistent method.

B. Molecular spin-orbit interaction

We will now consider the molecular spin-orbit interaction. The calculations of $\zeta_{t_2t_2}$ and ζ_{et_2} have been detailed in Ref. 21. We will briefly recall the main results.

For the monoelectronic wave functions e and t_2, the relevant matrix elements of τ are

$$\zeta_{t_2t_2} = -i\langle t_2\xi|\tau_z|t_2\eta\rangle = (a^d a^d - a^p a^p)\zeta_M + a^{\pi p}(\sqrt{2}a^{\sigma p} - a^{\pi p}/2)\zeta_L \tag{24}$$

and

$$\zeta_{et_2} = \frac{i}{2}\langle e\varepsilon|\tau_z|t_2\zeta\rangle = a^d b^d \zeta_M + b^{\pi p}(\sqrt{2}a^{\sigma p} + a^{\pi p})\zeta_L/2\sqrt{3}. \tag{25}$$

We can note here that in the CF model: $\zeta_{t_2t_2}=\zeta_{et_2}=\zeta_M$.

The spin-orbit coupling constants for the electrons $3d$ and $4p$ of Mn and for the electrons np of S, Se, and Te have been calculated following the method proposed by Blume and Watson.[38] We get $\zeta_M(\mathrm{Mn}:\ 3d,4p)=286.0+47.0(Q_M-1)$, $\zeta_L(\mathrm{S}:\ 3p)=297.7+65.3(Q_L+1)$, $\zeta_L(\mathrm{Se}:\ 4p)=1353.0+297.0(Q_L+1)$, and $\zeta_L(\mathrm{Te}:5p)=3444.0+756.0(Q_L+1)$.

C. One electron molecular dipole moment

In order to calculate the matrix elements of the electric dipole moment, the molecular orbitals t_2 and e are taken as linear combinations of the orbitals of Mn and of the group orbitals of the first four neighbors. Direct axis systems are used in order to avoid any phase problem during the calculations, in particular for the orbitals σp.

The matrix elements $z_{t_2t_2}$ and z_{et_2} are obtained as follows:

$$z_{t_2t_2} = \langle t_2\xi|z|t_2\eta\rangle = \sum_i\sum_j a^{Oi}a^{Oj}\langle O_i t_2\xi|z|O_j t_2\eta\rangle, \tag{26}$$

$$z_{et_2} = \langle e\varepsilon|y|t_2\eta\rangle = -\frac{\sqrt{3}}{2}\langle e\theta|z|t_2\zeta\rangle = -\frac{\sqrt{3}}{2}\sum_i\sum_j b^{O_i}a^{O_j}\langle O_i e\theta|z|O_j t_2\zeta\rangle. \tag{27}$$

For the state t_2, $i=1-5$ corresponds to the orbitals $3d$ and $4p$ of the cation and σst_2, σpt_2, πpt_2 of the ligands. For the state e, $k=1,2$ corresponds to the orbitals $3d$ of the metal and πp of the ligands. The group orbitals $O_i t_2 \gamma$ and $O_k e \gamma'$ are defined in Ref. 30.

It can be noted here that the calculation of the matrix elements of the electric dipole moments is much more difficult to handle than the calculation of the MSO interaction. The fundamental reason is that, in the case of the MSO interaction, the interaction is localized on the metal and on the ligands so that it is possible to decompose the MSO Hamiltonian into two terms acting either on the electrons of the metal or of the ligands, while in the case of the dipole moment, no such localization and simplification exists, so that, the calculation of the dipole moment **r** must be performed on the whole molecule thus seriously complicating the calculation.

Therefore, in order to check the theoretical results, three methods have been used to calculate the relevant matrix elements $\langle O_i t_2 \xi | z | O_j t_2 \eta \rangle$ and $\langle O_i t_2 \zeta | z | O_k e \theta \rangle$ of the electric dipole moments.

In the first method, described by Sharma,[39] the orbitals of the ligands are expressed in the axis system of the metal. For each ligand k, the atomic function χ whose spherical coordinates (R_k, Θ_k, Φ_k) are given in the axis system (O_{Lk}, x_k, y_k, z_k) is expressed in terms of a linear combination of wave functions α_l whose spherical coordinates (r, θ_k, φ_k) are expressed in the axis system $((O_M, x_k', y_k', z_k')$ centered on the metal. The axes associated to the metal and each ligand are parallel. Therefore, $\varphi_k = \phi_k$.

The wave function of the ligand k can be written as

$$\chi(NLM, R_k \Xi k_k \varphi_k) = \frac{1}{R_k} f_{NL}(R_k) Y_L^M(\Xi_k, \varphi_k) = \sum_{l=M}^{\infty} \frac{1}{r} \alpha_l(NLM|ar) Y_l^M(\theta_k, \varphi_k), \quad (28)$$

where Y_L^M and Y_l^M are spherical harmonics. r and R_k are the distances from the metal and from the ligand k respectively. $\alpha_l(NLM|ar)$ is a radial component of the development of the wave function χ of the ligand. It is given by

$$\alpha_l(NLM|ar) = \frac{1}{a} \int_0^{2\pi} \int_{|a-r|}^{a+r} f_{NL}(R_k) \times Y_L^M(\Xi_k, \varphi_k) Y_l^{M*}(\theta_k, \varphi_k) dR_k d\varphi_k. \quad (29)$$

For given values for NLM and l, then, α_l depends on **r** only.

The atomic wave function of the k ligand is obtained in the axis system (O_M, x'_k, y'_k, z'_k) of the metal, then, a rotation gives the development of χ in the axis system (O_M, x, y, z).

For the ligands, the wave functions e and t_2 are linear combinations of the atomic orbitals of the four ligands. By summing the contributions of the four ligands, we get the development of the wave functions e and t_2 of the ligands in the crystal axis system (O_M, x, y, z):

$$|O_j t_2 \zeta\rangle = \sum_{l=M}^{\infty} |O_j t_2 \zeta\rangle_l \quad (30)$$

and

$$|O_j e \theta\rangle = \sum_{l=M}^{\infty} |O_j e \theta\rangle_l, \quad (31)$$

where $M=0$ for the orbitals σs and σp and $M=1$ for the orbitals πp. For σs and σp, the term $l=0$ is zero when the summation is performed on the four ligands. Therefore, the development in α_l of the orbitals of the ligands contains terms l from 1 to ∞. The matrix elements of the component z of **r** are thus calculated for two molecular orbitals expressed in the common crystal axis system.

This method is well adapted for the calculation of the matrix elements of **r** involving the wave functions of the metal and of the ligands. However, when calculating ligand-ligand matrix elements of **r**, it is necessary to use a development involving high values for l in order to obtain convergent values for **r**. Therefore, in order to calculate the ligand-ligand matrix elements of **r**, it is better to use the following method.

The second method is the "overlap integrals method" described by Mulliken *et al.*[40] It permits us to calculate the metal-metal, the metal-ligand, and ligand-ligand matrix elements of z. The metal-ligand matrix elements of the component z of **r** are considered as the overlap integrals between the orbitals of the metal (bra) and the kets given by the operator z acting on the orbitals of the ligands. The kets are calculated in the axis system of the ligands. These matrix elements are calculated by using the method developed by Mulliken *et al.*[40] to calculate the overlap integrals.

This method permits a better insight in the physical interpretation of the results since it gives the contributions of each orbital of the metal and of the ligands. In particular, it clearly shows the influence of the metal-ligand distance. This method is convenient to calculate the metal-metal and the ligand-same-ligand matrix elements of z. However, it is very tedious when applied to the calculation of the ligand-other-ligand matrix elements of z since it involves complex rotations of axes systems. The ligand-other-ligand matrix elements of z have been calculated by using the following method.

In the third method, the matrix elements of the dipole moment are calculated numerically by decomposing the volume occupied by the molecule into elementary volumes and calculating the matrix elements for each elementary volume. Of course, this method does not permit to analyze the contributions of each molecular orbital to the RL's and also implies long calculation time.

V. RESULTS AND DISCUSSION

A. Matrix elements of the MSO interaction and of the electric dipole moment

Table II gives the relevant coefficients intervening in the molecular calculations.[21,22] The theoretical values are given

TABLE II. Values for the metal-ligand distance a, the Madelung constant C_{Mad}, the charges Q_{lat}, QM, QL, the cubic field parameter $D_{q\mathrm{calc}}$, and the SO coupling coefficients $\zeta_M(\mathrm{Mn})$ and $\zeta_L(L)$ as defined in Sec. V A.

Compounds	a (a.u.)	C_{Mad}	Q_{lat}	Q_M	Q_L	$D_{q\mathrm{calc}}$	$\zeta_M(\mathrm{Mn})$	$\zeta_L(L)$
ZnS (a)	4.41	1.63	0.8	1.313	0	−365	301	302
ZnS (b)	4.41	1.40	0.8	1.024	−0.856	−419	287	307
ZnS (c)	4.41	1.40	0.9	1.031	−0.933	−387	287	302
ZnS (d)	4.56	1.40	0.8	0.973	−0.843	−419	285	308
ZnSe (a)	4.61	1.63	0.7	1.219	−0.830	−310	296	1404
ZnSe (b)	4.61	1.40	0.7	0.981	−0.770	−378	285	1421
ZnSe (c)	4.76	1.40	0.7	0.935	−0.759	−386	283	1425
ZnSe (d)	4.76	1.25	0.7	0.740	−0.710	−456	274	1439
ZnTe (a)	5.00	1.63	0.6	1.056	−0.736	−312	289	3643
ZnTe (b)	5.00	1.63	0.7	1.083	−0.796	−278	290	3598
ZnTe (c)	5.00	1.63	0.7	1.014	−0.779	−305	287	3611
ZnTe (d)	5.11	1.63	0.7	1.050	−0.788	−293	288	3605

for the charge Q_M of the metal, the cubic field parameter $D_{q\mathrm{calc}}$, and the SO coupling constants $\zeta_M(\mathrm{Mn})$ of the d electrons of the metal and $\zeta_L(L)$ of the p electrons of the ligands. These values are obtained for slightly different values for the metal-ligand distance a, the charge of the lattice Q_{lat} and the Madelung constant CMad.

Figure 3 shows the calculated monoelectronic molecular energy levels in the case of ZnS set (a). Table III gives the calculated values for $z_{t_2t_2}$, z_{et_2}, $\zeta_{t_2t_2}$, and ζ_{et_2} for the four sets of parameters given in Table II. We can note that $\zeta_{t_2t_2}$ is positive for ZnS, negative for ZnSe, and large and negative for ZnTe. The values for $\zeta_{et_2}$are positive for all compounds and decrease when passing from the ligand S to ligands Se and Te. These values are to be compared with the value of approximately 300 cm^{-1} as given by the CF model.

For $z_{t_2t_2}$, it must be noted that, for all compounds, the values are very sensitive to the molecular coefficients used for the sets a, b, c, and d. The values of z_{et_2} slightly increase when passing from the ligand S to ligands Se and Te, and are larger than the values obtained for $z_{t_2t_2}$. This increase is due to the increasing value of the metal-ligand distance.

For ZnS, sets a and d, Table IV gives examples of the detailed metal-metal, metal-ligand and ligand-ligand contributions to $z_{t_2t_2}$ and z_{et_2}. These contributions to $z_{t_2t_2}$ and z_{et_2} are either positive or negative, so that, the precision of the overal values strongly depends on the precision of the mo-

TABLE III. Values for the monoelectronic matrix elements $\zeta_{t_2t_2}$, ζ_{et_2} of the MSO interaction and of the monoelectronic matrix elements $z_{t_2t_2}$ and z_{et_2} of the z component of the electric dipole moment.

Compounds	$\zeta_{t_2t_2}$ (cm^{-1})	ζ_{et_2} (cm^{-1})	$z_{t_2t_2}$ (10^{-8} cm)	z_{et_2} (10^{-8} cm)
ZnS (a)	178.0	236.0	0.028347	0.203848
ZnS (b)	130.6	210.0	0.063498	0.227478
ZnS (c)	138.8	210.2	0.066660	0.217716
ZnS (d)	131.0	205.0	0.098602	0.219391
ZnSe (a)	−139.3	193.5	0.032373	0.225694
ZnSe (b)	−250.3	161.9	0.066935	0.246648
ZnSe (c)	−233.0	149.3	0.101423	0.238553
ZnSe (d)	−321.0	125.0	0.135119	0.244565
ZnTe (a)	−876.8	102.0	0.059675	0.258452
ZnTe (b)	−801.3	105.4	0.055486	0.251195
ZnTe (c)	−878.3	88.0	0.070384	0.257090
ZnTe (d)	−774.3	82.0	0.084089	0.243941

TABLE IV. Contributions of the group orbitals O_i and O_j to $z_{t_2t_2}$ and z_{et_2} pour ZnS (a) and ZnS (b). The group orbitals are defined in Sec. IV A.

Orbitals			ZnS (a) (10^{-8} cm)		ZnS (d) (10^{-8} cm)	
$z_{t_2t_2}$	$\langle O_i t_2 \xi \vert$	$\vert O_j t_2 \eta \rangle$		s/total		s/total
metal-metal	$3d$	$4p$	−0.0421		−0.0466	
				−0.0421		−0.0466
metal-ligand	$4p$	σs	0.0142		0.0178	
	$4p$	σp	0.0036		−0.0002	
	$4p$	πp	0.0269		0.0369	
	$3d$	σs	−0.0269		−0.0243	
	$3d$	σp	−0.0995		−0.1175	
	$3d$	πp	0.0280		0.0270	
				−0.0537		−0.0603
ligand-ligand	σs	σs	0.0233		0.0202	
	σs	σp	−0.0382		−0.0409	
	σs	πp	0.0179		0.0171	
	σp	σp	0.2119		0.3068	
	σp	πp	−0.0014		−0.0016	
	πp	πp	−0.0893		−0.0961	
				0.1241		0.2055
total for z_{et_2}				0.0283		0.0986
z_{et_2}	$\langle O_i e \varepsilon \vert$	$\vert O_j t_2 \varsigma \rangle$		s/total		s/total
metal-metal	$3d$	$4p$	0.0199		0.0224	
				0.0199		0.0224
metal-ligand	πp	$4p$	−0.0389		−0.0540	
	πp	$3d$	0.0000		0.0000	
	$3d$	πp	−0.0298		−0.0303	
	$3d$	σp	0.0295		0.0343	
	$3d$	σs	0.0060		0.0053	
				−0.0332		−0.0446
ligand-ligand	πp	σs	−0.0312		−0.0296	
	πp	σp	−0.0020		−0.0024	
	πp	πp	0.2504		0.2736	
				0.2171		0.2416
total for z_{et_2}				0.2038		0.2194

lecular wave functions. More precisely, for $z_{t_2t_2}$, the positive ligand-ligand contribution is partially compensated by the negative metal-metal and metal-ligand contributions. The positive σp-σp ligand-ligand contribution is preponderant, however, it is strongly reduced by the negative πp-πp ligand-ligand and $3d$-σp metal-ligand contributions. It can also be noted that $z_{t_2t_2}$ is very sensitive to the variations of the components $a^{\sigma p}$ and $a^{\pi p}$ of the $4t_2$ wave functions.

For z_{et_2} the metal-metal contribution is to a large extend compensated by the metal-ligand contribution, so that, z_{et_2} is primarily given by the πp-πp ligand-ligand contribution. z_{et_2} is proportional to the metal-ligand distance and to the product $a^{\pi p}b^{\pi p}$ of the πp components of the wave functions t_2 and e. $a^{\pi p}b^{\pi p}$ is not very sensitive to the sets of parameters a, b, c, d, or to the nature of the ligands.

B. Lifetimes of Mn^{2+} in ZnS, ZnSe, and ZnTe

From Sec. II, formula (1), the lifetimes are given by

$$\frac{1}{\tau} = 7.23543 \frac{\sigma^3 \chi}{d_A} (6f^2) \times 10^{10}, \tag{32}$$

where σ is the energy, in units of cm^{-1}, of the center of gravity of the experimental emission band of the fluorescent level. For ZnS, $\sigma = 17\,100\ cm^{-1}$,[41–43] for ZnSe, $\sigma = 17\,200\ cm^{-1}$,[44,45] for ZnTe, $\sigma = 15\,870\ cm^{-1}$.[46,47] d_A is the degeneracy of the excited state.

TABLE V. Values for f, τ_{HT}, and τ_{BT} for ZnS in (a), ZnSe and ZnTe in (b). Three sets of values for B, C, and D_q have been considered in the case of ZnS. We have taken $B=740\ cm^{-1}$, $C=2740\ cm^{-1}$, $D_q=-405\ cm^{-1}$ for ZnSe (Ref. 44) and $B=628\ cm^{-1}$, $C=2824\ cm^{-1}$, $D_q=-434\ cm^{-1}$ for ZnTe (Ref. 46).

	a									
	$B=730\ cm^{-1}$[a] $C=2880\ cm^{-1}$ $D_q=-420\ cm^{-1}$			$B=630\ cm^{-1}$[b,c] $C=3040\ cm^{-1}$ $D_q=-520\ cm^{-1}$			$B=830\ cm^{-1}$[d] $C=2500\ cm^{-1}$ $D_q=-450\ cm^{-1}$			
	f (10^{-11} cm)	τ_{HT} (μs)	τ_{BT} (μs)	f (10^{-11} cm)	τ_{HT} (μs)	τ_{BT} (μs)	f (10^{-11} cm)	τ_{HT} (μs)	τ_{BT} (μs)	Experimental[e,f] value τ_{exp}(μs)
ZnS (a)	1.674	1336	1214	1.632	1405	1278	1.819	1132	1029	1770 (at 4.2 K)
ZnS (b)	1.079	3213	2921	1.023	3576	3251	1.198	2606	2369	
ZnS (c)	1.030	3530	3209	0.975	3937	3579	1.138	2890	2627	
ZnS (d)	0.634	9305	8459	0.569	11557	10506	0.715	7330	6663	
	b									
	f (10^{-11} cm)	τ_{HT} (μs)	τ_{BT} (μs)	$\tau_{texp.}$ (μs)						
ZnSe (a)	−0.776	5350	4863	220–240[g,h] (at 4 K)						
ZnSe (b)	−2.153	696	633							
ZnSe (c)	−2.198	668	607							
ZnSe (d)	−3.147	326	296							
ZnTe (a)	−8.557	38	34	40–52[i] (at 10 K)						
ZnTe (b)	−7.586	48	44							
ZnTe (c)	−8.557	38	34							
ZnTe (d)	−7.192	53	48							

[a]Reference 17.
[b]Reference 42.
[c]Reference 43.
[d]Reference 14.
[e]Reference 3.
[f]Reference 4.
[g]Reference 5.
[h]Reference 6.
[i]Reference 7.

As shown in the Introduction, the fluorescent $^4T_1$ level consists of two groups of two lines separated by $\Delta=-9.5\ cm^{-1}$ for ZnS and $\Delta=-11.5\ cm^{-1}$ for ZnSe.[48] In the case of ZnS, a small splitting of $0.6-0.7\ cm^{-1}$ has been observed for the lines at lower and at higher energy.[49] These splittings, which cannot be explained by the CF-model have been accounted for from a molecular model corresponding to the sets b and d for the molecular coefficients.[14]

For ZnS and ZnSe, at high temperature ($T \gg 15$ K) all zero phonon levels of the $^4T_1$ fluorescent levels are populated so that $d_A=12$. A low temperature ($T \ll 15$ K), the levels at lower energy are the only ones to be populated so that $d_A=6$. Since the theoretical RDS's of the two lines [Γ_7 and $\Gamma_8(3/2)$] at lower energy and of the two lines [$\Gamma_8(5/2)$ and Γ_6] at higher energy are 11 and 9, respectively, the lifetime at low temperature is 10/11 of the lifetime at high temperature.

χ gives the effective electric field with respect to the macroscopic field in the coumpound. $\chi=n(n^2+2)^2/9$ with $n^2=\varepsilon^\infty$. In ZnS, $\varepsilon^\infty=5.52$,[50] in ZnSe, $\varepsilon^\infty=5.9$,[51] and in ZnTe, $\varepsilon^\infty=7.18$.[52]

Table V gives f, τ_{HT}, and τ_{BT}, for ZnS, ZnSe, and ZnTe. Three sets of values for B, C, and D_q have been considered in the case of ZnS in order to analyze the influence of slight variations of the multielectronic wave functions on the RL's. One set of values for ZnSe and for ZnTe have been considered. Except for one set of values for ZnS:Mn which was obtained by fitting the energies of zero phonon lines, the others values for B, C, and D_q have been obtained by fitting the energies of the absorption bands at lower energy of Mn^{2+}. It must be noted that f is positive for ZnS and negative for ZnSe and ZnTe and that its sign is primarily controlled by $\zeta_{t_2t_2}$.

Concerning the RL's of $ZnS:Mn^{2+}$, Table V a shows that sets a, b, and c give theoretical values for τ_{BT} (from 1.03 to 3.58 ms when considering the three sets for B, C, and D_q) which are in agreement with the experimental value of 1.77 ms at 4.2 K. Set d gives large values from 6.66 ms to 8.46 and 10.51 ms for the three sets for B, C, and D_q.

We can briefly recall here the results obtained from sets a to d in previous molecular models for the SLCC G_{11} of the fundamental $^6A_1$ level to E strains and for the OLCC $V_E(^4T_1)$ of the fluorescent level to E strains.

For G_{11} ($ZnS:Mn^{2+}$), the very small and negative experimental value of $-0.02\ cm^{-1}$ has been correctly accounted for

from sets *c* and *d*, while sets *a* and *b* have predicted positive values for G_{11}.[21] (The theoretical values for G_{11} are of 0.116, 0.013, −0.005, and −0.002 cm^{-1}, for sets *a*, *b*, *c*, and *d*, respectively.) It must be noted that in the case of ZnS, the theoretical values for G_{11} depend on large and almost equal contributions of opposite signs, so that, the magnitude and the sign of G_{11} is very sensitive to the structure of the molecular wave functions.

For $V_E(^4T_1)$ ($ZnS:Mn^{2+}$), the experimental value of −10 700 cm^{-1} has been correctly accounted for by all sets, the theoretical values being of −8760 cm^{-1}, −9385 cm^{-1}, −9335 cm^{-1}, and −8430 cm^{-1} for sets *a*, *b*, *c*, and *d*, respectively.[22]

For $ZnSe:Mn^{2+}$, Table V b shows that: set a gives a very large theoretical value of 4863 μs for τ_{BT}, the experimental value being of 220–240 μs at 4.2 K; sets *b* and *c* give values for τ_{BT} (633 and 607 μs, respectively) which are in rough agreement with the experimental value; for set *d*, the theoretical value of 296 μs is in excellent agreement with the experimental value. It can be noted that this set *d* gives the best agreement for G_{11}.[21] More precisely, the theoretical values for G_{11} are of 0.94, 0.70, 0.58, and 0.36 cm^{-1} for sets *a*, *b*, *c*, and *d*, respectively, the experimental value being of 0.34 cm^{-1}. For the OLCC $V_E(^4T_1)$, the experimental value of −10900 cm^{-1} is correctly accounted for by all sets, the theoretical values being of −7780, −8430, −7700, and −8270 cm^{-1} for sets *a*, *b*, *c*, and *d*, respectively.[22] For $ZnTe:Mn^{2+}$ Table V b shows that the theoretical values obtained from the four sets of monoelectronic wave functions are in excellent agreement with the experimental value of 40–52 μs.

C. Case of d^5 ions in II-VI and III-V compounds

In the case of Mn^{2+} and Fe^{3+} in II-VI and III-V compounds, it can be noted that, for a given cation, the RL's follow the general trend of a decrease of the RL's when increasing the SO coupling constants ζ_L of the *p* electrons of the ligands. This trend is verified for the RL's of Fe^{3+} in II-VI compounds which are of 25.2 ms in axial ZnO[9] and 4.3 ms in ZnS,[8] since, for effective charges of −1 for the ligands, ζ_L is approximately of 120 cm^{-1} for O^- and 300 cm^{-1} for S^-. It is also verified for the RL's of Fe^{3+} in III-V compounds which are of 8 ms in GaN[12] and 1.9 ms in GaAs,[10,11] since ζ_L is approximately of 55 cm^{-1} for N^-, and 985 cm^{-1} for As^-.

VI. CONCLUSION

A molecular model has been elaborated to account for the lifetimes of the fluorescent $^4T_1$ levels of d^5 ions in tetrahedral symmetry. The RL's have been calculated from second-order perturbation schemes involving the molecular SO interaction and the electric dipole moment. The matrix elements of H_{SO} and **r** have been calculated from four sets of slightly different monoelectronic wave functions and from multielectronic wave functions which were used to evaluate the OLCC's and SLCC's of Mn^{2+} in II-VI compounds. The electric dipole moment for the molecular system has been calculated from three different methods. Detailed contributions of the metal-ligand, ligand-ligand, and ligand-other-ligand have been analyzed in the case of ZnS.

It has been shown that the molecular model accounts for the drastic variations of one to almost two orders of magnitude of the RL's in the case of Mn^{2+} in the common cation series ZnS, ZnSe, and ZnTe. More precisely, for ZnS and also for ZnSe, three sets of monoelectronic wave functions used to calculate the OLCC's and SLCC's correctly accounted for the RL's, while one set has given too large values for the RL's. For ZnTe, the theoretical values as obtained from four slightly different sets of monoelectronic molecular wave functions have been found to be in excellent agreement with the experimental value. Finally, it must be noted that the RL's are correctly accounted for by restricting the molecular calculations to the three $^4T_1$ levels at lower energy and that the fundamental interaction which accounts for the strong decrease of the RL's of Mn^{2+} in ZnS, ZnSe, and ZnTe is the MSO interaction of the *p* electrons of the ligands.

ACKNOWLEDGMENTS

Thanks are due to A. Gélineau, C. Naud, and E. Bringuier for very helpful discussions on radiative lifetimes of impurities in crystals.

[1] W. Busse, H. E. Gumlich, A. Geoffroy, and R. Parrot, Phys. Status Solidi B **93**, 591 (1979).
[2] W. Busse, H. E. Gumlich, W. Knack, and J. Schulze, J. Phys. Soc. Jpn. **49**, 581 (1980).
[3] H. E. Gumlich (private communication).
[4] T. C. Leslie and J. W. Allen, Phys. Status Solidi A **65**, 545 (1981); S. G. Ayling and J. W. Allen, J. Phys. C **20**, 4251 (1987).
[5] W. Gebhardt (private communication).
[6] A. Hoffmann, R. Heitz, and I. Broser, Phys. Rev. B **41**, 5806 (1990).
[7] R. Heitz, A. Hoffmann, and I. Broser, Phys. Rev. B **45**, 8977 (1992).
[8] K. Pressel, G. Bohnert, G. Rückert, A. Dörnen, and K. Thonke, J. Appl. Phys. **71**, 5703 (1992).
[9] K. Pressel, G. Rückert, A. Dörnen, and K. Thonke, Phys. Rev. B **46**, 13 171 (1992).
[10] R. Heitz, P. Thurian, I. Loa, L. Eckey, A. Hoffmann, I. Broser, K. Pressel, B. K. Meyer, and E. N. Mokhov, Appl. Phys. Lett. **67**, 2822 (1995).
[11] K. Pressel, G. Bohnert, A. Dörnen, B. Kaufmann, J. Denzel, and K. Thonke, Phys. Rev. B **47**, 9411 (1993).
[12] R. N. Bhargava, D. Gallagher, X. Hong, and A. Nurmikko, Phys. Rev. Lett. **72**, 416 (1994).
[13] B. A. Smith, J. Z. Zhang, A. Joly, and J. Liu, Phys. Rev. B **62**, 2021 (2000).

[14] D. Boulanger and R. Parrot, Phys. Rev. B **66**, 205201 (2002).
[15] J. Schneider, S. R. Sircar, and A. Räuber, Z. Naturforsch. A **18**, 980 (1963).
[16] C. Kikuchi and G. H. Azarbayejani, J. Phys. Soc. Jpn. **17**, 453 (1962); H. H. Woodbury and G. W. Ludwig, Bull. Am. Phys. Soc. **6**, 118 (1961).
[17] R. Parrot and C. Blanchard, Phys. Rev. B **5**, 819 (1972); **6**, 3992 (1972).
[18] R. Parrot, Phys. Rev. B **9**, 4660 (1974).
[19] T. Hoshina, J. Phys. Soc. Jpn. **48**, 1261 (1980).
[20] D. Boulanger, D. Curie, and R. Parrot, J. Lumin. **48/49**, 680 (1991).
[21] R. Parrot and D. Boulanger, Phys. Rev. B **47**, 1849 (1993).
[22] D. Boulanger and R. Parrot, J. Chem. Phys. **87**, 1469 (1987).
[23] W. Beall Fowler and D. L. Dexter, Phys. Rev. **128**, 2154 (1962).
[24] F. S. Ham, Phys. Rev. **138**, A1727 (1965); G. A. Slack, F. S. Ham, and R. M. Chrenko, Phys. Rev. **152**, 376 (1966).
[25] A. Gélineau, Ph.D. thesis, University of Paris VI, 1972.
[26] R. Parrot, C. Naud, and F. Gendron, Phys. Rev. B **13**, 3748 (1976).
[27] A. A. Misetich and T. Buch, J. Chem. Phys. **41**, 2524 (1964).
[28] J. S. Griffith, *The Irreducible Tensor Method for Molecular Symmetry Groups* (Prentice Hall, Englewood Cliffs, NJ, 1962).
[29] S. Sugano, Y. Tanabe, and H. Kamimura, *Multiplets of Transition Metal Ions in Crystals* (Academic, New York, 1970).
[30] See, for example, C. J. Ballhausen and H. B. Gray, *Molecular Orbital Theory* (Benjamin, New York, 1965); H. Basch, A. Viste, and H. B. Gray, Theor. Chim. Acta **3**, 458 (1965).
[31] T. Buch and A. Gelineau, Phys. Rev. B **4**, 1444 (1971).
[32] J. W. Richardson, R. R. Powell, and W. C. Nieuwpoort, J. Chem. Phys. **36**, 1057 (1962); **38**, 796 (1963).
[33] R. E. Watson and A. J. Freeman, Phys. Rev. **123**, 521 (1961); **124**, 1117 (1961).
[34] E. Clementi, IBM J. Res. Dev. **9**, 2 (1965).
[35] H. Basch, A. Viste, and H. B. Gray, Theor. Chim. Acta **3**, 458 (1965).
[36] C. E. Moore, Natl. Bur. Stand. Circ. (U. S.) **467** (1952).
[37] L. C. Cusachs, J. Chem. Phys. **43**, S157 (1965).
[38] M. Blume and R. E. Watson, Proc. R. Soc. London, Ser. A **271**, 565 (1963).
[39] R. R. Sharma, Phys. Rev. A **13**, 517 (1976).
[40] R. S. Mulliken, C. A. Rieke, D. Orloff, and H. Orloff, J. Chem. Phys. **17**, 1248 (1949).
[41] D. Langer and S. Ibuki, Phys. Rev. **138**, A809 (1965).
[42] T. Kushida, Y. Tanaka, and Y. Oka, Solid State Commun. **14**, 617 (1974).
[43] J. Dreyhsig and J. W. Allen, J. Phys.: Condens. Matter **1**, 1087 (1989).
[44] D. Langer and H. S. Richter, Phys. Rev. **146**, 554 (1966).
[45] J. Dreyhsig, U. Stutenbäumer, and H. E. Gumlich, J. Cryst. Growth **101**, 443 (1990).
[46] J. E. Morales Toro, W. M. Becker, B. I. Wang, U. Debska, and J. W. Richardson, Solid State Commun. **52**, 41 (1984).
[47] M. Skowronski, J. M. Baranowski, and L. J. Ludwicki, Akad. Nauk (PAN) **75**, 127 (1978).
[48] R. Parrot, C. Naud, C. Porte, D. Fournier, A. C. Boccara, and J. C. Rivoal, Phys. Rev. B **17**, 1057 (1978).
[49] R. Parrot, D. Boulanger, and M. N. Diarra, Phys. Rev. B **54**, 1662 (1996).
[50] S. Ozaki and S. Adachi, J. Appl. Phys. **32**, 5008 (1993).
[51] D. T. F. Marple, J. Appl. Phys. **35**, 539 (1964).
[52] K. Kunc, M. Balkanski, and M. A. Nusimovici, Phys. Status Solidi B **72**, 229 (1975).